ELSEVIER

Journal of Chromatography A, 934 (2001) 31–49

JOURNAL OF CHROMATOGRAPHY A

www.elsevier.com/locate/chroma

Flux of gases across the air–water interface studied by reversed-flow gas chromatography

Khan Atta Rashid, Dimitrios Gavril, Nicholas A. Katsanos, George Karaiskakis*

Department of Chemistry, University of Patras, GR-26504 Patras, Greece

Received 20 July 2001; received in revised form 6 September 2001; accepted 6 September 2001

Abstract

In the present work the reversed-flow gas chromatographic technique was applied for the study of flux of gases across the air–water interface. The model system was vinyl chloride–water, which is of great significance in food and environmental chemistry. Using suitable mathematical analysis, equations were derived by means of which the following physicochemical quantities were calculated: diffusion coefficient of vinyl chloride (VC) into water, partition coefficient of VC between the water (at the interface and the bulk) and the carrier gas nitrogen, overall mass transfer coefficients of VC in the gas (nitrogen) and the liquid (water), gas and liquid film transfer coefficients of VC, gas and liquid phase resistances for the transfer of VC into the water, and finally the thickness of the stagnant film in the liquid phase, according to the two-film theory of Whitman. From the variation of the above parameters with temperature, as well as the volume and the free surface area of the water, useful conclusions concerning the mechanism for the transfer of VC into water were extracted. These are discussed in comparison with the same parameters calculated from empirical equations or determined experimentally by other techniques.
© 2001 Elsevier Science B.V. All rights reserved.

Keywords: Air–water interface; Reversed-flow gas chromatography; Diffusion coefficients; Partition coefficients; Mass transfer; Vinyl chloride

1. Introduction

The description and quantification of the physical and chemical phenomena controlling the exchange of chemicals between the atmosphere and water bodies are of great significance in environmental chemistry [1,2]. The approach is first to describe the several physical processes which may apply simultaneously as a chemical migrates between these phases. Based on this conceptual ''model'', equations can be derived describing the various processes and manipulated into convenient forms for applying to real situations in which the aim is to predict transfer rates. These equations contain equilibrium and kinetic parameters or coefficients which normally require separate determination. In some cases the coefficients can be estimated indirectly or obtained from correlations. As the total resistance to the exchange of any gas between air and water is a combination of the resistances in the gaseous and liquid phases [1–4], a method measuring individual resistances should be of great significance. For this particular purpose, the relatively new technique of reversed-

*Corresponding author. Tel.: +30-61-997-144; fax: +30-61-997-144.

E-mail address: g.karaiskakis@chemistry.upatras.gr (G. Karaiskakis).

0021-9673/01/$ – see front matter © 2001 Elsevier Science B.V. All rights reserved.
PII: S0021-9673(01)01277-8

flow gas chromatography was used, which gives information not only on phase equilibria, but also on interface transport across the air–water boundaries [5–9].

Reversed-flow gas chromatography (RF-GC) consists of reversing the direction of flow of the carrier gas from time to time. If other gases are contained in the carrier gas and their concentration depends on a rate process within the chromatographic column, each flow reversal creates a perturbation in the chromatographic elution curve in the form of extra peaks (termed ''sample peaks''). Then, by repeatedly reversing the flow of the carrier gas, a repeated sampling of this rate process is performed.

RF-GC has been used to determine gas diffusion coefficients in binary and ternary mixtures [10,11], adsorption equilibrium constants [12], molecular diameters and critical volumes of gases [13], Lennard–Jones parameters [14], activity coefficients [15]. mass transfer coefficients on solids and liquids [6–9], solubility and interaction parameters [16], rate constants, activation parameters and conversions of the reactants into products for various important surface-catalysed reactions [17–19], as well as rate constants for the sorption processes of various gases on bimetallic catalysts [20,21]. In two recent reviews [22,23], some other advances in physico-chemical measurements of the method are described.

In the present work the model of vinyl chloride–water interaction was selected as vinyl chloride is related to the primary group of toxic chemical carcinogens and has received considerable attention both in terms of residual levels in the plastic and as a consequent contaminant in foods [24,25]. Although the model developed has been applied to the vinyl chloride–water system, it should be possible to use it at any air–water interface in the environment.

2. Experimental

2.1. Materials

Vinyl chloride (VC) of 99.99% purity from Matheson Gas Products was used as solute, while the carrier gas was nitrogen of 99.99% purity from BOC Gases.

2.2. Apparatus and procedure

The experimental setup is schematically outlined in Fig. 1. It was basically that described elsewhere [6,7] except for the geometry of the glass vessel in which the water was placed. The surface area (a_L) and the volume (V_L) of the water were the two parameters which were varied in the present work. The gaseous volumes V_G (the gas volume in column L_1) and V'_G (the gas volume in vessel y above the liquid) were measured by filling the columns with water at a certain temperature, weighing them, and using the density of the water at that temperature. All geometrical characteristics of the cells used in the experiments are given in Table 1.

After the injection of 1 cm^3 of VC at atmospheric pressure, a continuous concentration–time curve is recorded passing through a maximum and then declining with time. By means of a six-port valve, the carrier gas flow direction is reversed for 5 s, which is a shorter time period than the gas hold-up time in both column sections l and l', and then the gas is again turned to its original direction. This procedure creates extra chromatographic peaks (sample peaks) superimposed on the continuous elution curve (cf. Fig. 2). This is repeated many times during the experiment lasting a few hours. The height H of the sample peaks from the continuous signal, taken as baseline, to their maximum is plotted as $\ln H$ versus time, giving a *diffusion band*, whose shape and slope both depend on whether the vessel L_2 is empty or contains water, as well as on the geometric characteristics of the vessel and the temperature.

In all experiments, the pressure drop along $l + l'$ was negligible, while the carrier gas flow-rate was kept constant (1.0 $cm^3\ s^{-1}$) and the working temperature was in the range 317.70–346.00 K.

3. Theory

The height H of each sample peak (cf. Fig. 2) above the ending baseline is proportional to the concentration $c(l', t)$ of the solute (vinyl chloride) in the sampling column at $x = l'$ and at time t (cf. Fig. 1) [6,7,26]:

$$H = 2c(l', t) \quad (1)$$

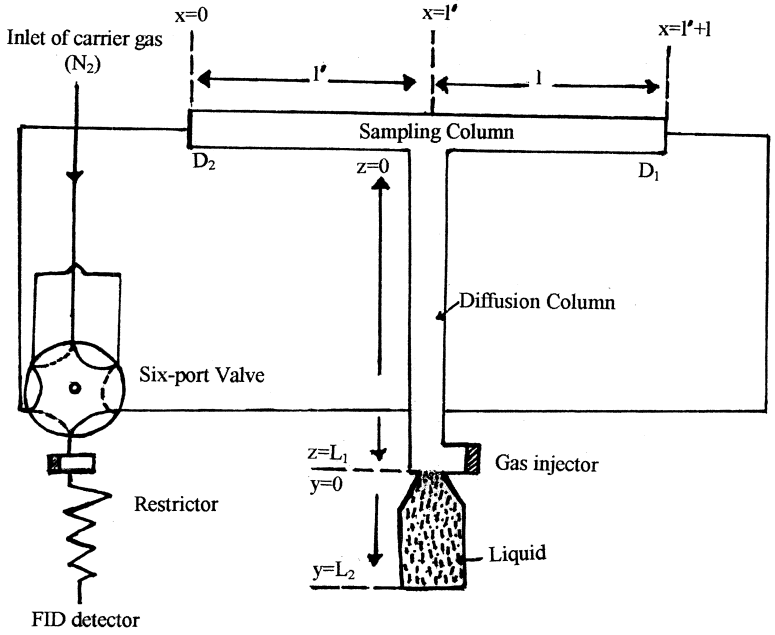

Fig. 1. Schematic representation of the reversed-flow gas chromatographic technique for studying the flux of gases across the air–water interface. FID detector, flame ionization detector.

It has been shown previously [6,7] that when the lower part L_2 of the diffusion column (cf. Fig. 1) is empty, the height of the sample peaks, H, after the maximum of the diffusion band, is given by:

$$H = \frac{6mD_G}{\dot{V}L_1^2(1 + 3V'_G/V_G)} \cdot \exp\left(- \frac{3D_G/L_1^2}{1 + 3V'_G/V_G} t \right) \quad (2)$$

where D_G is the diffusion coefficient of VC into the carrier gas nitrogen, m is the amount of VC injected (mol), V_G and V'_G are the gaseous volumes in sections L_1 and L_2 of the diffusion column, respectively, and $\dot{V}$ is the volumetric flow-rate of the carrier gas. Eq. (2) shows that a plot of $\ln H$ versus t (after the maximum) is linear during the whole experiment with a slope equal to $-(3D_G/L_1^2)/(1 + 3V'_G/V_G)$, from which the D_G parameter can be calculated, as all the rest quantities are known.

When the lower part L_2 of the diffusion column is filled with quiescent water, and the distribution

Table 1
Geometrical characteristics of the cells used in the present work

Data	First series of experiments (E1)	Second series of experiments (E2)	Third series of experiments (E3)	Fourth series of experiments (E4)
L_1 (cm)	42.0	44.0	43.7	42.7
L_2 (cm)	3.0	3.0	2.6	2.6
a_G (cm^2)	0.2177	0.2177	0.2177	0.2177
a_L (cm^2)	0.2334	0.0600	0.2334	0.0600
V_G (cm^3)	9.14	9.58	9.51	9.34
V'_G (cm^3)	4.43	4.43	0.32	0.32
V_L (cm^3)	4.43	4.43	0.32	0.32

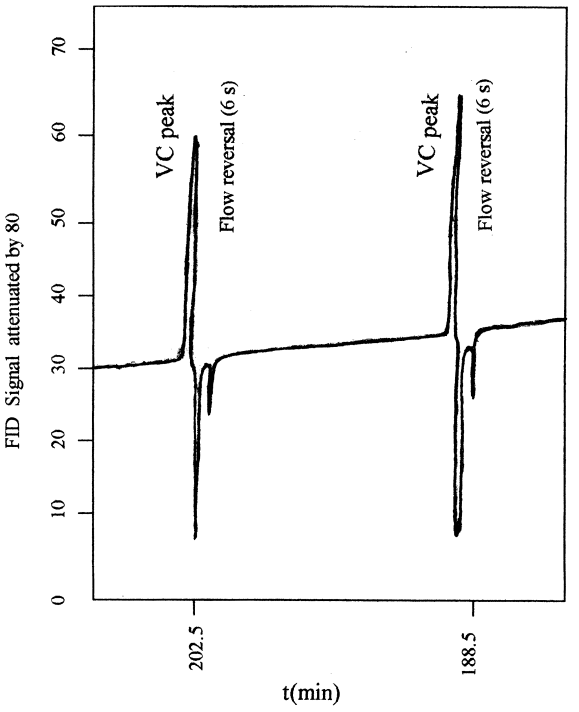

Fig. 2. A reversed-flow gas chromatograph showing two sample peaks for the adsorption of vinyl chloride by water at 345.85 K and 1 atm ($V_L = 0.32$ cm^3, $a'_L = 0.0600$ cm^2).

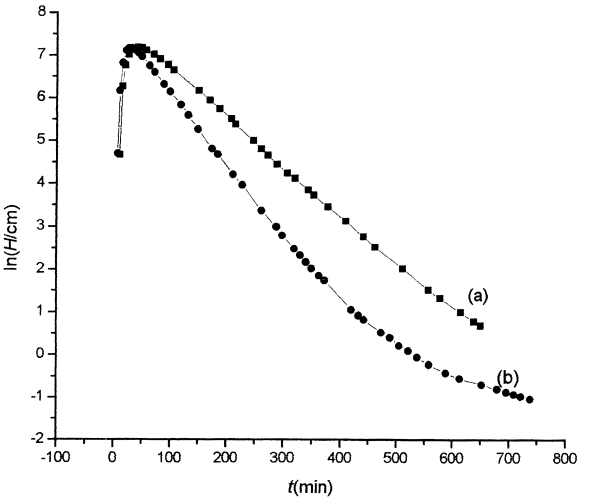

Fig. 3. Plot of ln H versus t for the adsorption of VC by water at two temperatures: (a) $T = 317.70$ K; (b) $T = 345.845$ K ($V_L = 0.32$ cm^3, $a'_L = 0.0600$ cm^2).

equilibrium of VC between the gas nitrogen and the water is rapidly established, the diffusion band (after the maximum) remains linear (cf. Fig. 3a), but its slope changes and Eq. (2) is modified as follows [6,7]:

$$H = \frac{6mD_G}{\dot{V}L_1^2(1 + 3V'_G/V_G)} \cdot \exp\left(-\frac{3D_G/L_1^2}{1 + 3(1+\kappa)V'_G/V_G}t \right) \quad (3)$$

where κ is the partition ratio of VC between the water and nitrogen.

When the distribution equilibrium of the VC between the gas and the liquid is established slowly, the diffusion band (after the maximum) is no longer linear, but distorted, as shown in Fig. 3b. A new mathematical treatment for the extraction of the relevant equation describing the descending part of this distortion is presented in the present work, which starts from Eq. (15) of Ref. [9]:

$$C(l', p) = \frac{m}{a_G D_G q_1} \cdot \left[\sinh q_1 L_1 + \frac{v}{D_G q_1} \cdot \cosh q_1 L_1 + K \cdot \frac{a_L D_L q_2}{a_G D_G q_1} \cdot \tanh q_2 L_2 \left(\cosh q_1 L_1 + \frac{v}{D_G q_1} \cdot \sinh q_1 L_1 \right) \right]^{-1} \quad (4)$$

where a_G, a_L are cross-sectional areas in gas diffusion column and liquid column, respectively (cm^2); D_G, D_L are diffusion coefficients in gas and liquid, respectively (cm^2/s); $K = c_y(0)/c_z(L_1)$ is partition coefficient, dimensionless; L_1, L_2 are diffusion lengths in gaseous and liquid regions, respectively (cm); $q_1^2 = p/D_G$, $q_2^2 = p/D_L$; v is linear velocity of carrier gas (cm/s); $C(l', p)$ is Laplace transformed concentration $c(l', t)$, at the junction of diffusion and sampling column.

New approximations, different from those of Ref. [9], are used in the equation which results, after the omission in Eq. (4) of sinh q_1L_1 and cosh q_1L_1

compared to $(v/D_G q_l)\cosh q_1 L_1$ and $(v/D_G q_1)\sinh q_1 L_1$, respectively:

$$C(l', p) = \frac{m}{a_G D_G q_1} \cdot \left[\frac{v}{D_G q_1} \cdot \cosh q_1 L_1 + K \cdot \frac{a_L D_L q_2}{a_G D_G q_1} \cdot \tanh q_2 L_2 \left(\frac{v}{D_G q_1} \cdot \sinh q_1 L_1 \right) \right]^{-1} \quad (5)$$

Algebraic manipulations of Eq. (5) lead to

$$C(l', p) = \frac{mA}{\dot{V}} \cdot \frac{\cosh q_2 L_2}{A \cosh q_1 L_1 \cdot \cosh q_2 L_2 + KJ \sinh q_1 L_1 \cdot \sinh q_2 L_2} \quad (6)$$

where

$$A = \frac{a_G}{a_L}, \dot{V} = v a_G \quad \text{and} \quad J = \frac{D_L q_2}{D_G q_1} = \frac{D_L^{1/2}}{D_G^{1/2}} \quad (7)$$

Both cosh qL and sinh qL functions are expanded in McLaurin series in qL, retaining only the first two non-zero terms in each of them, namely:

$$\cosh q_1 L_1 = 1 + \frac{q_1^2 L_1^2}{2}, \quad \cosh q_2 L_2 = 1 + \frac{q_2^2 L_2^2}{2} \quad (8)$$

$$\sinh q_1 L_1 = q_1 L_1 + \frac{q_1^3 L_1^3}{3!}, \quad \sinh q_2 L_2 = q_2 L_2 + \frac{q_2^3 L_2^3}{3!} \quad (9)$$

Substitution of Eqs. (8) and (9) in Eq. (6) and use of the relations $q_1^2 = p/D_G$, $q_2^2 = p/D_L$ and Eq. (7), gives, after collection of same powers of p, the relation:

$$C(l', p) = \frac{18mAD_G^2}{K\dot{V}L_1^3 L_2} \cdot \frac{p + 2D_L/L_2^2}{p^3 + Xp^2 + Yp + Z} \quad (10)$$

where

$$X = \frac{9AD_G}{KL_1 L_2} + \frac{6D_G}{L_1^2} + \frac{6D_L}{L_2^2} \quad (11)$$

$$Y = \frac{18AD_G^2}{KL_1^3 L_2} + \frac{18AD_G D_L}{KL_1 L_2^3} + \frac{36D_G D_L}{L_1^2 L_2^2} \quad (12)$$

$$Z = \frac{36AD_G^2 D_L}{KL_1^3 L_2^3} \quad (13)$$

If the roots of the polynomial in the denominator of Eq. (10) are B_1, B_2 and B_3, this is written:

$$C(l', p) = \frac{18mAD_G^2}{K\dot{V}L_1^3 L_2} \cdot \frac{p + 2D_L/L_2^2}{(p - B_1)(p - B_2)(p - B_3)} \quad (14)$$

and the roots are related to the coefficients X, Y and Z by:

$$X = -(B_1 + B_2 + B_3) \quad (15)$$

$$Y = B_1 B_2 + B_1 B_3 + B_2 B_3 \quad (16)$$

$$Z = -B_1 B_2 B_3 \quad (17)$$

Inverse transformation of Eq. (14) with respect to p, and combination with Eq. (1), gives

$$\frac{H}{2} = c(l', t) = A_1 \exp(B_1 t) + A_2 \exp(B_2 t) + A_3 \exp(B_3 t) \quad (18)$$

where the pre-exponential coefficients A_1, A_2 and A_3 can be written as explicit functions of B_1, B_2, B_3, the geometrical characteristics of the cell and other experimental quantities, but this is not needed for the following calculations. Thus, from the pairs H, t of the experiment, the coefficients A_1, B_1, A_2, B_2, A_3, B_3 are found by non-linear least-squares regression analysis, as described in Ref. [26].

From B_1, B_2 and B_3, the values of X, Y and Z are found according to Eqs. (11), (12) and (13). From these, the D_L and K are calculated as follows.

From Eq. (13), one obtains

$$\frac{D_G D_L}{K} = \frac{ZL_1^3 L_2^3}{36AD_G} \quad (19)$$

and this, substituted into Eq. (12), gives

$$Y = \frac{18AD_G^2}{L_1^3 L_2} \cdot \frac{1}{K} + \frac{ZL_1^2}{2D_G} + \frac{36D_G D_L}{L_1^2 L_2^2} \quad (20)$$

Multiplying Eq. (11) by $2D_G/L_1^2$, and subtracting the result from Eq. (20), the K is removed:

$$Y - \frac{2D_G X}{L_1^2} = \frac{ZL_1^2}{2D_G} - \frac{12D_G{}^2}{L_1^4} + \frac{24D_G}{L_1^2 L_2^2} D_L \tag{21}$$

By using the known value of D_G, as it was determined when the vessel L_2 was empty, the D_L is calculated from the above, by the relation

$$D_L = \left(Y - \frac{2D_G X}{L_1^2} - \frac{ZL_1^2}{2D_G} + \frac{12D_G{}^2}{L_1^4} \right) \cdot \frac{L_1^2 L_2^2}{24D_G} \tag{22}$$

Then, substitution of D_L into Eqs. (19) or (20) gives K.

The Henry's law constant, H^+, can be calculated by using the approximation

$$H^+ = \frac{RTd}{KM_L} \tag{23}$$

where d is the density of the liquid, and M_L its molar mass.

For the calculation of the overall mass transfer coefficients in gases, K_G (cm s^{-1}), and liquids, K_L(cm s^{-1}), we started from Eq. (28) of Ref. [8], supposing again that we can omit sinh qL and cosh qL, compared to v/Dq(cosh qL) and v/Dq (sinh qL), respectively:

$$C(l', p) = \frac{m}{a_G D_G q} \cdot \left[\frac{v}{Dq} \cdot \cosh qL + \frac{kp}{Dq(p + k')} \cdot \left(\frac{v}{Dq} \cdot \sinh qL \right) \right]^{-1} \tag{24}$$

where

$q^2 = p/D_G$, $L = L_1$ (gas phase)
$k = K_G a_L / a_G$, $k' = K_L a_L / V_L$ (liquid volume)

A new approximation was adopted also here, namely, three terms in the McLaurin series:

$$\cosh q_L = 1 + \frac{q^2 L^2}{2} + \frac{q^4 L^4}{4!},$$
$$\sinh qL = qL + \frac{q^3 L^3}{3!} + \frac{q^5 L^5}{5!} \tag{25}$$

After substitution of Eq. (25) in Eq. (24) and algebraic manipulations we obtain:

$$C(l', p) = \frac{24mD_G{}^2}{\dot{V}L^4(1 + kL/5D_G)} \cdot \frac{p + k'}{p^3 + X'p^2 + Y'p + Z'} = \frac{24mD_G{}^2}{\dot{V}L^4(1 + kL/5D_G)} \cdot \frac{p + k'}{(p - B_1)(p - B_2)(p - B_3)} \tag{26}$$

where

$$X' = -(B_1 + B_2 + B_3) = \frac{12D_G/L^2 + 4k/L + k'}{1 + kL/5D_G} \tag{27}$$

$$Y' = B_1B_2 + B_1B_3 + B_2B_3 = \frac{24D_G{}^2/L^4 + 24kD_G/L^3 + 12k'D_G/L^2}{1 + kL/5D_G} \tag{28}$$

$$Z' = -B_1B_2B_3 = \frac{24k'D_G{}^2/L^4}{1 + kL/5D_G} \tag{29}$$

Inversing Eq. (26) with respect to p, gives Eq. (18) from which A_1, B_1, A_2, B_2, A_3, B_3 are already known from the previous calculation of D_L and K. Thus, X', Y' and Z' are found. From these

$$\frac{X'}{Z'L^4} - \frac{Y'}{6D_G L^2 Z'} = \frac{1}{3L^2 D_G} \cdot \frac{1}{k'} - \frac{1}{24D_G{}^2} \tag{30}$$

and solving for $1/k'$:

$$\frac{1}{k'} = \left(\frac{X'}{Z'L^4} - \frac{Y'}{6D_G L^2 Z'} + \frac{1}{24D_G{}^2} \right) \cdot 3L^2 D_G \tag{31}$$

and

$$K_L = k'V_L/a_L \tag{32}$$

Then, substituting k' in Eq. (27), we find k, and from this:

$$K_G = ka_G/a_L \tag{33}$$

Because the total resistance (R) for the gas transfer expressed on a liquid phase basis ($1/K_L$) depends on the gas (k_G) and liquid (k_L) film transfer coefficients, according to the two-film theory of Whitman [1,4],

as well as on the value of the Henry's law constant (H^+) for the gas concerned or on the partition coefficient (K') of the gas (VC) between the water bulk and the carrier gas nitrogen, which is expressed as the ratio K_G/K_L, we need the equation relating the K_L with k_G, k_L and K' [1,4]:

$$\frac{1}{K_L} = \frac{1}{k_L} + \frac{K'}{k_G} \tag{34}$$

For convenience in using Eq. (34), $1/k_L$ may be written as r_L and K'/k_G as r_G:

$$R = r_L + r_G \tag{35}$$

The numerical values of r_L and r_G for any gas indicate the relative importance of liquid and gas phase resistance for exchange of that particular gas. As it is very difficult to measure individual resistances, it is very important to know the ratio r_L/r_G, which indicates which one of the two phase resistances controls the exchange. This can be done as follows: putting $K' = K_G/K_L$ in Eq. (34) and using the k_G value ($\approx$0.4474 cm s^{-1}) for vinyl chloride found in Ref. [1], we can find k_L. Then, from k_L and k_G, the r_L and r_G can be calculated, and from these the ratio r_L/r_G. Even the used k_G value is an approximation and independent of the temperature, we can use it as we are not interested in the absolute values of the resistances r_L and r_G, but, as was mentioned earlier, mainly in their ratio, r_L/r_G.

Finally, from the known relation

$$z_L = \frac{D_L}{k_L} \tag{36}$$

and knowing the D_L and k_L parameters, one obtains the very important quantity of the thickness of the stagnant film in the liquid phase, z_L, while from the ratio K/K', one obtains the partition coefficient of the gas between the water at the interface and the bulk, K''.

$$K'' = \frac{K}{K'} \tag{37}$$

As regards homogeneity in concentrations from the stagnant films, the diffusion coefficients in the gas phase, at the working temperature, are high enough to ensure a satisfactory homogeneity in that phase. On the other hand, the diffusion coefficients in the liquid phase are so small, that during the period of the experimental measurements they are unable to create important heterogeneities in the liquid. Therefore, the final conclusions drawn from the results, do not seem to be influenced by heterogeneity in either phase.

4. Results and discussion

As pointed out in Section 3, the following physicochemical quantities, describing the flux of gases across the air–water interface, can be determined by using the reversed-flow gas chromatography technique:

(i) Diffusion coefficient of the gas into the carrier gas nitrogen (D_G, cm^2 s^{-1}).

(ii) Diffusion coefficient of the gas into the water (D_L, cm^2 s^{-1}).

(iii) Partition coefficient of the gas between the water at the interface and the carrier gas nitrogen (K, dimensionless).

(iv) Partition coefficient of the gas between the water bulk and the carrier gas nitrogen (K', dimensionless).

(v) Partition coefficient of the gas between the water at the interface and the bulk (K'', dimensionless).

(vi) Henry's law constant for the dissolution of the gas into the water (H^+, atm; 1 atm = 101 325 Pa).

(vii) Overall mass transfer coefficients of the gas in the gas nitrogen (K_G, cm s^{-1}) and in the liquid water (K_L, cm s^{-1}).

(viii) Gas (k_G, cm s^{-1}) and liquid (k_L, cm s^{-1}) film transfer coefficients, according to the two-film theory of Whitman.

(ix) Gas (r_G, s cm^{-1}) and liquid (r_L, s cm^{-1}) phase resistances for the transfer of the gas into the water.

(x) Thickness of the stagnant film in the liquid phase (z_L, cm).

The model system was vinyl chloride–water, while the experimental parameters varied were the temperature, as well as the volume and the free surface area of the liquid water (cf. Table 1). We performed four series of experiments (El, E2, E3 and E4) at various temperatures and the data for the experimental arrangements used are presented in

Table 2
Diffusion coefficients of VC into nitrogen, D_G, partition coefficients of VC between the water interface and nitrogen, K, Henry's law constants for the dissolution of VC into water, H^+, diffusion coefficients of VC into water, D_L, overall mass transfer coefficients of VC into the water, K_L, and nitrogen, K_G, water film transfer coefficients of VC, k_L, water, r_L, and nitrogen, r_G, resistances for the transfer of VC into water, ratios r_L/r_G, thicknesses of the stagnant films in the water, z_L, as well as partition coefficients of VC between the water bulk and nitrogen, K', and partition coefficients of VC between the water at the interface and the bulk, K'', at various temperatures and at two water-free surface areas, $a_L = 0.2334$ cm^2 (E1 experiments) and $a'_L = 0.0600$ cm^2 (E2 experiments)

T (K)	D_G (cm^2 s^{-1})	K	H^+ (atm)	$10^4\ D_L$ (cm^2 s^{-1})	$10^3\ K_L$ (cm s^{-1})	$10^4\ K_G$ (cm s^{-1})	K'	$10^3\ k_L$ (cm s^{-1})	$10^2\ z_L$ (cm)	r_L (s cm^{-1})	r_G (s cm^{-1})	r_L/r_G	K''
E1 experiments													
324.05	0.140	11.22	129.87	2.679	4.648	6.777	0.146	4.655	5.755	214.83	0.3259	659.19	77.00
329.05	0.143	13.32	110.90	2.586	5.170	6.389	0.124	5.178	4.994	193.13	0.2762	699.24	107.75
339.55	0.152	13.46	112.55	5.176	3.382	15.490	0.458	3.394	15.254	294.65	1.0237	287.83	29.40
345.55	0.157	12.65	121.45	6.177	3.657	20.646	0.565	3.674	16.811	272.15	1.2617	215.70	22.42
E2 experiments													
324.40	0.140	65.98	22.11	2.767	11.130	17.893	0.161	11.175	2.470	89.48	0.3593	249.04	410.48
329.00	0.143	38.23	38.62	1.657	20.196	18.065	0.089	20.278	0.082	49.31	0.1998	246.80	427.62
334.65	0.147	47.00	31.87	2.094	18.491	18.342	0.099	18.568	1.127	53.86	0.2215	243.16	474.30
339.35	0.151	44.67	33.92	2.500	19.209	28.276	0.147	19.331	1.292	51.73	0.3290	157.23	303.44
345.90	0.158	32.66	47.13	4.233	33.636	28.961	0.086	33.614	1.259	29.75	0.1920	154.95	379.77

The water volume was kept constant in all experiments ($V_L = 4.43$ cm^3).

Table 1. In all cases, except from one shown in Fig. 3a, the diffusion band after the maximum is no linear, indicating that the distribution equilibrium of VC between the gas and the liquid is established slowly. Comparison of the results obtained by experiments El and E2, as well as by experiments E3 and E4, shows the influence of the liquid (water)–free surface area (a_L or a'_L) on the physicochemical quantities measured, as the volume of the liquid is kept constant in both cases ($V_L = 4.43$ cm^3 in the first case and $V'_L = 0.32$ cm^3 in the second case). Likewise, comparison of the results obtained by experiments E1 and E3, as well as by experiments E2 and E4, shows the influence of the volume of the liquid (V_L or V'_L) on the parameters which will be found, as the liquid surface area is kept constant in both cases

Table 3
Thermodynamic and kinetic parameters for the transfer of VC into water at various temperatures and at two water-free surface areas, $a_L = 0.2334$ cm^2 (E3 experiments) and $a'_L = 0.0600$ cm^2 (E4 experiments)

T(K)	D_G (cm^2 s^{-1})	K	H^+ (atm)	$10^4\ D_L$ (cm^2 s^{-1})	$10^3\ K_L$ (cm s^{-1})	$10^4\ K_G$ (cm s^{-1})	K'	$10^3\ k_L$ (cm s^{-1})	$10^2\ z_L$ (cm)	r_L (s cm^{-1})	r_G (s cm^{-1})	r_L/r_G	K''
E3 experiments													
324.25	0.140	16.63	87.68	3.034	1.682	1.066	6.339	1.686	1.800	5932.61	14.167	418.63	2.624
328.90	0.144	12.85	114.85	2.821	2.445	1.127	4.612	2.451	1.151	4080.18	10.308	395.82	2.787
334.70	0.147	18.04	83.26	3.208	1.867	1.180	6.321	1.872	1.714	5342.06	14.129	378.11	2.854
339.30	0.151	17.99	84.19	3.518	2.083	1.438	6.903	2.089	1.683	4785.51	15.428	310.19	2.607
346.00	0.157	13.55	113.55	–	–	–	–	–	–	–	–	–	–
E4 experiments													
324.25	0.140	59.75	24.11	2.493	9.571	3.136	3.277	9.638	0.259	1037.54	7.324	141.67	18.236
328.80	0.143	47.53	31.06	1.560	17.719	2.955	1.668	17.837	0.087	560.62	3.727	150.42	28.501
334.50	0.148	72.11	20.76	2.665	9.627	3.200	3.324	9.696	0.275	1031.33	7.430	138.82	21.694
339.20	0.151	54.16	27.97	2.478	14.359	4.114	2.865	14.492	0.171	690.01	6.403	107.77	18.904
345.85	0.157	47.70	32.26	3.353	14.276	6.329	4.433	14.481	0.232	690.53	9.908	69.70	10.762

The water volume was kept constant in all experiments ($V'_L = 0.32$ cm^3). All parameters were defined in Section 3 and Table 2.

Table 4
Thermodynamic and kinetic parameters for the transfer of VC into water at various temperatures and at two water volumes, $V_L = 4.43$ cm^3 (E1 experiments) and $V'_L = 0.32$ cm^3 (E3 experiments)

T(K)	D_G (cm^2 s^{-1})	K	H^+ (atm)	$10^4\ D_L$ (cm^2 s^{-1})	$10^3\ K_L$ (cm s^{-1})	$10^4\ K_G$ (cm s^{-1})	K'	$10^3\ k_L$ (cm s^{-1})	$10^2\ z_L$ (cm)	r_L (s cm^{-1})	r_G (s cm^{-1})	r_L/r_G	K''
E1 experiments													
324.05	0.140	11.22	129.87	2.679	4.648	6.777	0.146	4.655	5.755	214.83	0.3259	659.19	77.00
329.05	0.143	13.32	110.90	2.586	5.170	6.389	0.124	5.178	4.994	193.13	0.2762	699.24	107.75
339.55	0.152	13.46	112.55	5.176	3.382	15.490	0.458	3.394	15.254	294.65	1.0237	287.83	29.40
345.55	0.157	12.65	121.45	6.177	3.657	20.646	0.565	3.674	16.811	272.15	1.2617	215.70	22.42
E3 experiments													
324.25	0.140	16.63	87.68	3.034	1.682	1.066	6.339	1.686	1.800	5932.61	14.167	418.63	2.624
328.90	0.144	12.85	114.85	2.821	2.445	1.127	4.612	2.451	1.151	4080.18	10.308	395.82	2.787
334.70	0.147	18.04	83.26	3.208	1.867	1.180	6.321	1.872	1.714	5342.06	14.129	378.11	2.854
339.30	0.151	17.99	84.19	3.518	2.083	1.438	6.903	2.089	1.683	4785.51	15.428	310.19	2.607
346.00	0.157	13.55	113.55	–	–	–	–	–	–	–	–	–	–

The water-free surface area was kept constant in all experiments ($a_L = 0.2334$ cm^2). All parameters were defined in Section 3 and Table 2.

($a_L = 0.2334$ cm^2 in the first case and $a'_L = 0.0600$ cm^2 in the second case). It must be pointed out that we also performed one series of experiments with empty the vessel L_2, so as to calculate the diffusion coefficients of VC into the carrier gas nitrogen.

The physicochemical quantities found in the present work for the transfer of VC into water at various temperatures and at two free surfaces areas and volumes of water are listed in Tables 2–5. From these values and their variation with temperature and the liquid-free surface area and volume (see representative plots in Figs. 4–11), the following conclusions can be drawn.

4.1. Variation with temperature

(1) The diffusion coefficients of VC into N_2, D_G, increase with temperature, as the theory predicts. (2) The partition coefficients of VC between the water at interface and nitrogen, K, decrease with temperature, due to the decreased concentration of VC at the water interface with temperature, as a consequence of the increased concentration of VC at the water bulk with temperature, which results from the fact that the solubility of VC into the water bulk increases with temperature. (3) The partition coefficients of VC between the water bulk and nitrogen,

Table 5
Thermodynamic and kinetic parameters for the transfer of VC into water at various temperatures and at two water volumes, $V_L = 4.43$ cm^3 (E2 experiments) and $V'_L = 0.32$ cm^3 (E4 experiments)

T(K)	D_G (cm^2 s^{-1})	K	H^+ (atm)	$10^4\ D_L$ (cm^2 s^{-1})	$10^3\ K_L$ (cm s^{-1})	$10^4\ K_G$ (cm s^{-1})	K'	$10^3\ k_L$ (cm s^{-1})	$10^2\ z_L$ (cm)	r_L (s cm^{-1})	r_G (s cm^{-1})	r_L/r_G	K''
E2 experiments													
324.40	0.140	65.98	22.11	2.767	11.130	17.893	0.161	11.175	2.470	89.48	0.3593	249.04	410.48
329.00	0.143	38.23	38.62	1.657	20.196	18.065	0.089	20.278	0.082	49.31	0.1998	246.80	427.62
334.65	0.147	47.00	31.87	2.094	18.491	18.342	0.099	18.568	1.127	53.86	0.2215	243.16	474.30
339.35	0.151	44.67	33.92	2.500	19.209	28.276	0.147	19.331	1.292	51.73	0.3290	157.23	303.44
345.90	0.158	32.66	47.13	4.233	33.636	28.961	0.086	33.614	1.259	29.75	0.1920	154.95	379.77
E4 experiments													
324.25	0.140	59.75	24.41	2.493	9.571	3.136	3.277	9.638	0.259	1037.54	7.324	141.67	18.236
328.80	0.143	47.53	31.06	1.560	17.719	2.955	1.668	17.837	0.087	560.62	3.727	150.42	28.501
334.50	0.148	72.11	20.76	2.665	9.627	3.200	3.324	9.696	0.275	1031.33	7.430	138.82	21.694
339.20	0.151	54.16	27.97	2.478	14.359	4.114	2.865	14.492	0.171	690.01	6.403	107.77	18.904
345.85	0.157	47.70	32.26	3.353	14.276	6.329	4.433	14.481	0.232	690.53	9.908	69.70	10.762

The water-free surface area was kept constant in all experiments ($a'_L = 0.2600$ cm^2). All parameters were defined in Section 3 and Table 2.

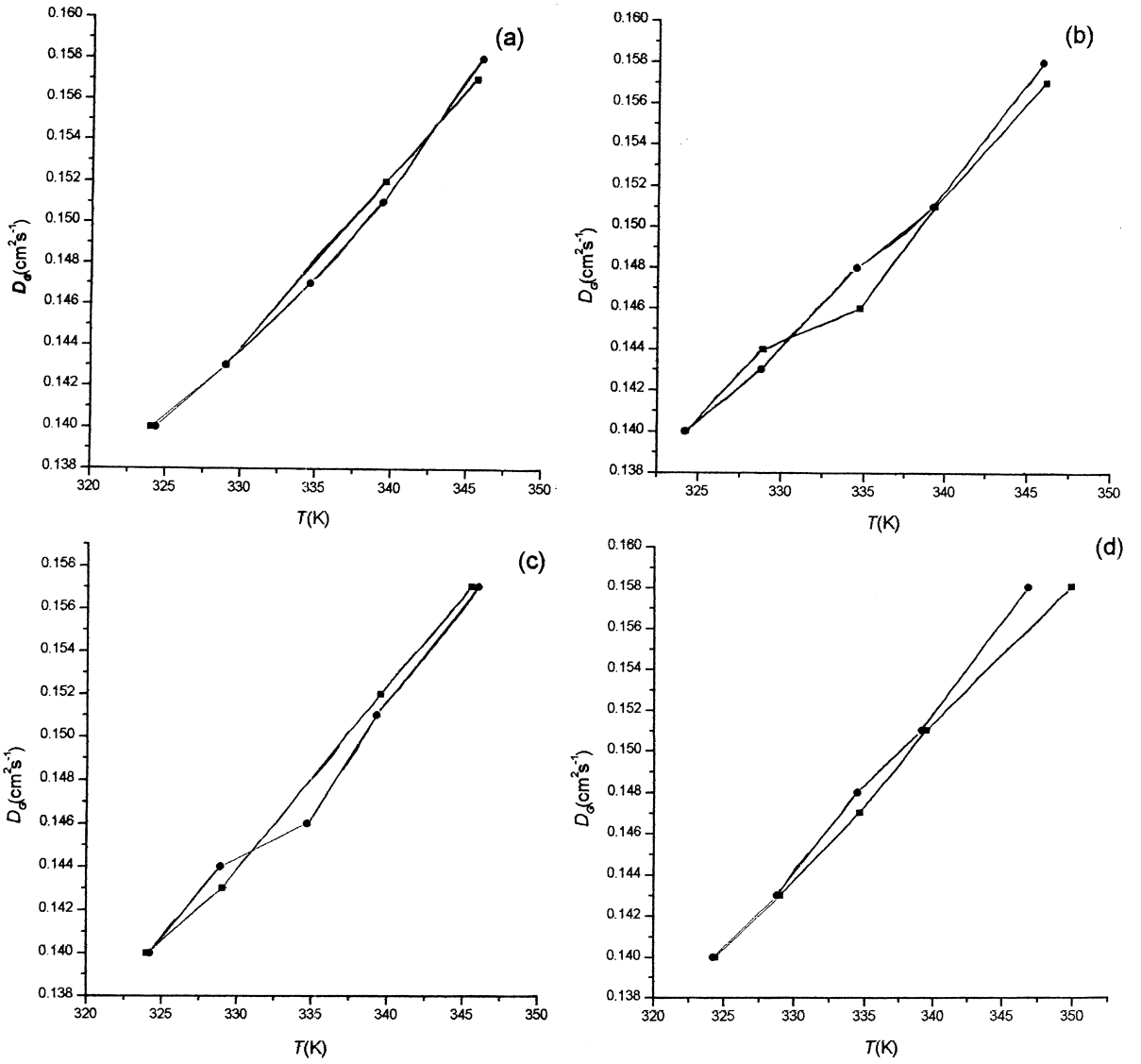

Fig. 4. Variation of the diffusion coefficients of VC into nitrogen (D_G) with temperature (T) at two different water-free surface areas, $a_L = 0.2334$ cm^2 (■) and $a_L' = 0.0600$ cm^2 (●), and at a constant water volume, $V_L = 4.43$ cm^3 (a) and $V_L' = 0.32$ cm^3 (b), as well as at two different volumes of water, V_L, $= 4.43$ cm^3 (■) and $V_L' = 0.32$ cm^3 (●), and at a constant water-free surface area, $a_L = 0.2334$ cm^2 (c) and $a_L' = 0.0600$ cm^2 (d).

K', increase with temperature, due to the increased concentration of VC at the water bulk with temperature. (4) The partition coefficients of VC between the water at the interface and the bulk, K'', decrease with temperature, as $K'' = K/K'$. This can be attributed to the fact that while the concentration of VC at the water bulk increases with temperature, the same concentration of VC at the water interface decreases with temperature. (5) The Henry's law constants, H^+, for the dissolution of VC at the water interface, generally, increase with temperature, due to the decreased concentration of VC at the water interface with temperature. (6) The diffusion coefficients of VC into water, D_L, increase with temperature, as the

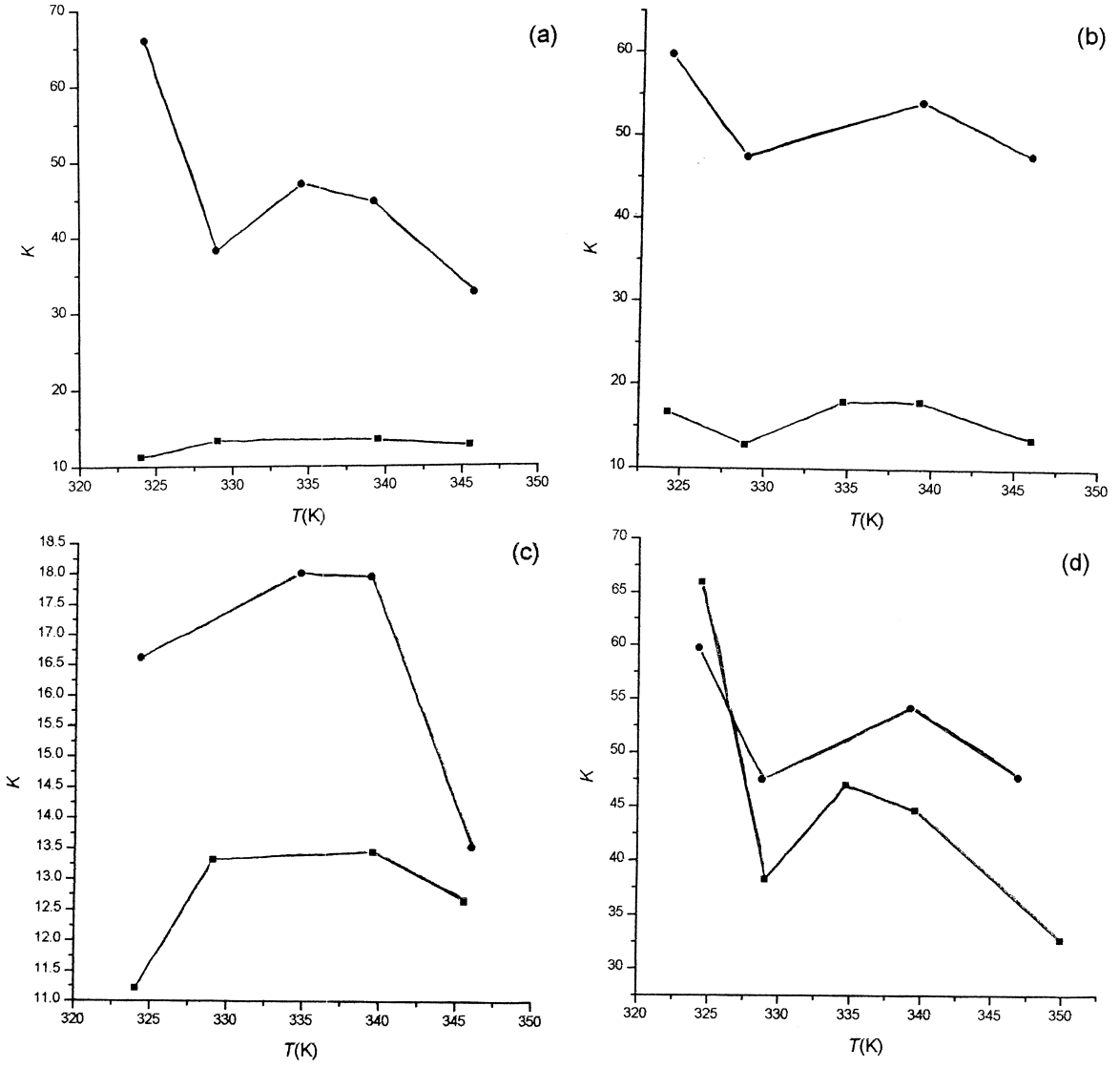

Fig. 5. Temperature dependence of partition coefficients of VC between the water interface and nitrogen (K). Cases (a)–(d), as well as the symbols of the experimental points in this and in the following figures correspond to those given in Fig. 4.

theory predicts. (7) The overall mass transfer coefficients of VC in the liquid (water) phase, K_L, generally, increase with temperature, as K_L is proportional to D_L ($K_L = \pi^2 D_L V_L / 4L_2^2 a_L$). It must be pointed out that the decrease of K_L with temperature observed in few cases can be attributed to accidental errors. (8) The overall mass transfer coefficients of VC in the gas (nitrogen) phase, K_G, increase with temperature, as $K_G = K' K_L$, and both K' and K_L increase with temperature. (9) The liquid film transfer coefficients of VC, k_L, increase with temperature, as a consequence of the increase of K_L with temperature, as K_L is proportional to k_L. (10) The thickness of the stagnant films in the liquid phase, z_L, generally, decreases with temperature, although in some cases an anomalous behaviour is observed, as a consequence of the same behaviour of K_L and k_L, which can be also attributed to accidental errors.

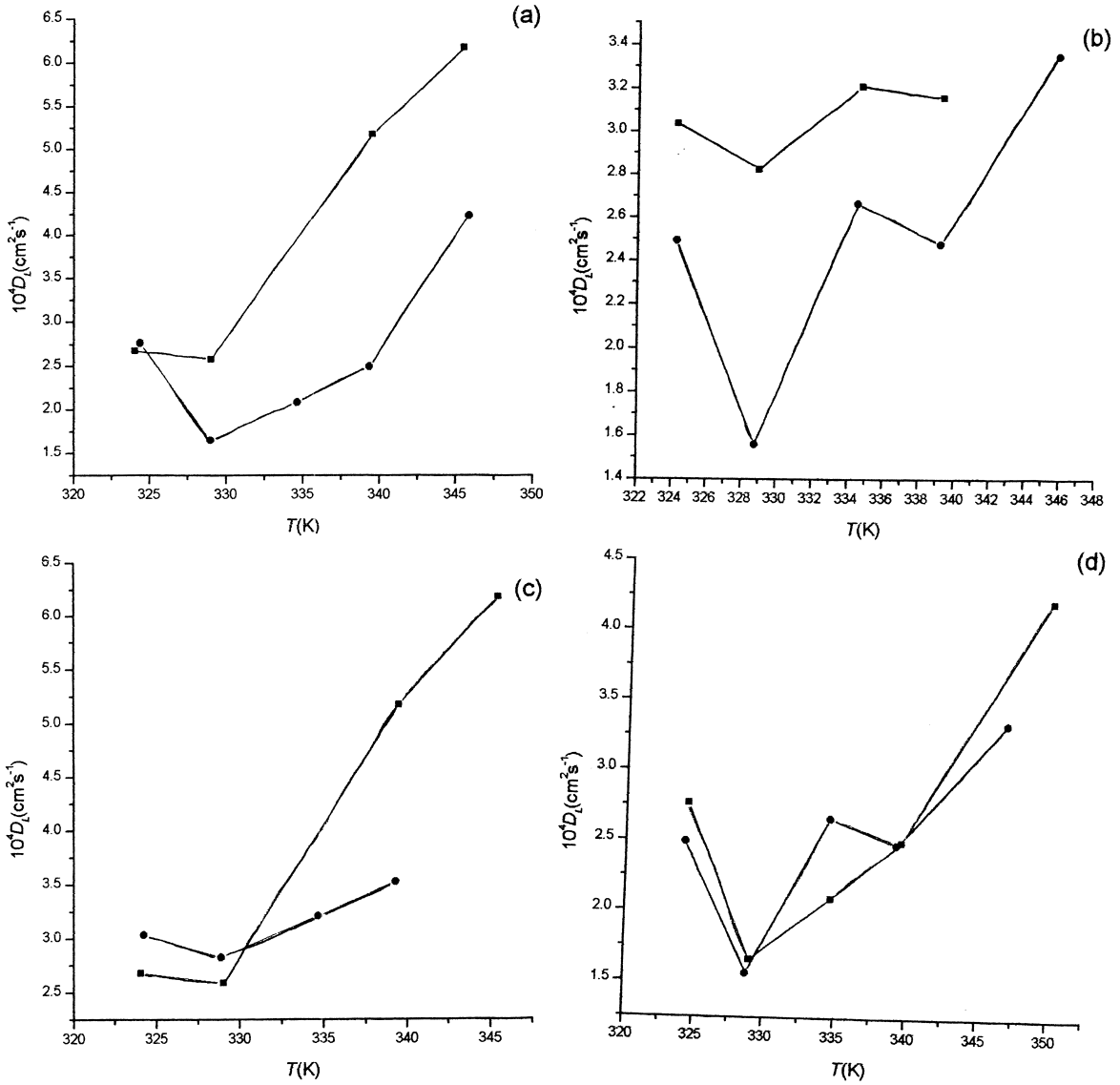

Fig. 6. Variation of diffusion coefficient of VC into water (D_L) with temperature.

Considering that $z_L = D_L/k_L$, as well as that both D_L an k_L increase with temperature, in order that z_L decreases with temperature, the rhythm of increase of k_L with temperature must be higher from that of D_L with temperature. (11) The liquid phase resistance of VC, r_L, decreases with temperature, as $r_L = 1/k_L$, and k_L increases with temperature. Physically, this means that the transfer of VC into water becomes easier at higher temperatures, as the liquid phase resistance, which controls this process, decreases with temperature. (12) The gas phase resistance of VC, r_G, increases with temperature, as $r_G = K'/k_G$ and K' increases with temperature, while k_G supposed to be constant ($k_G = 0.4474$ cm s^{-1}, the value found in Ref. [1]) and independent of temperature. (13) The ratio r_L/r_G decreases with temperature

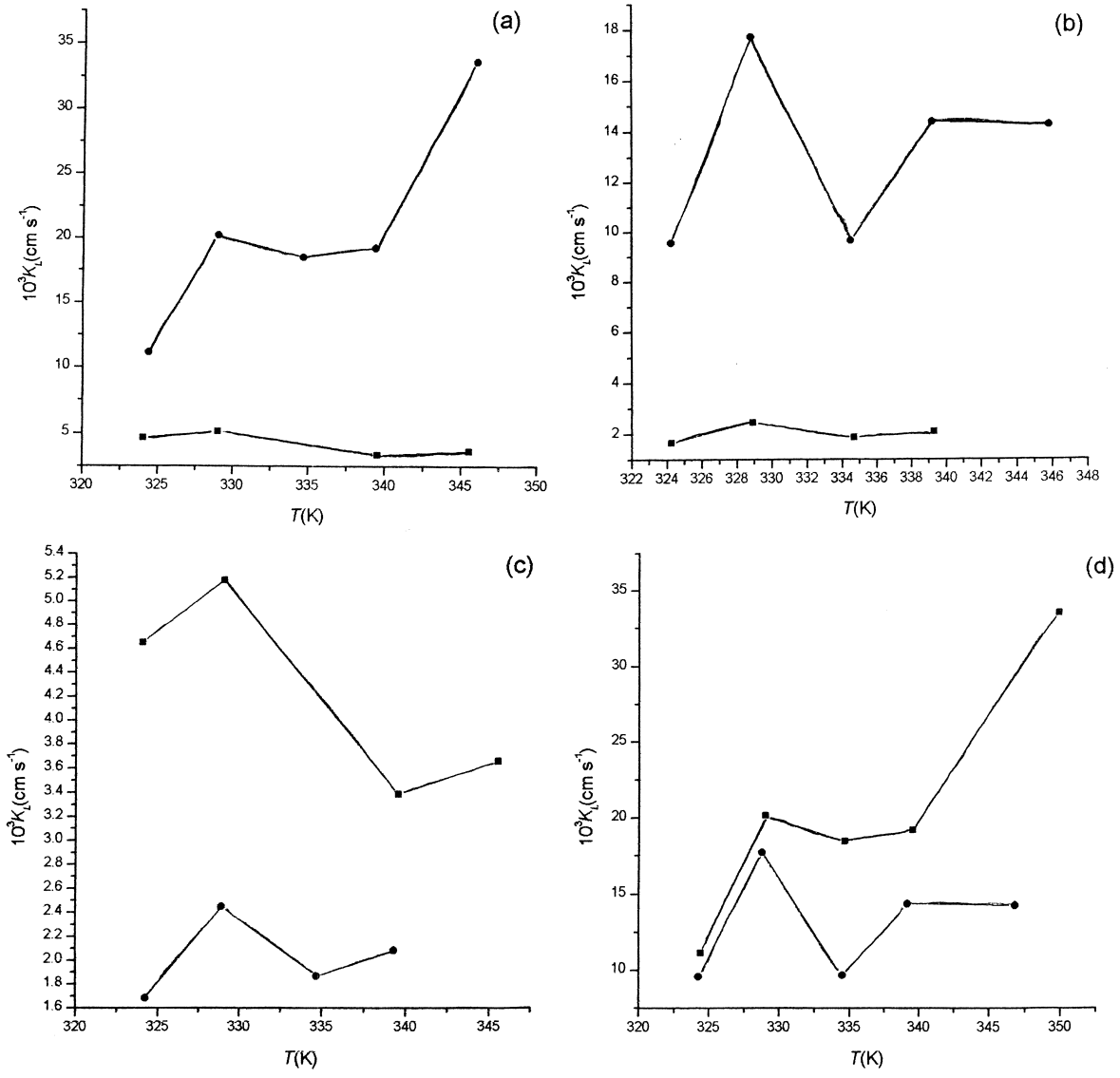

Fig. 7. Variation of overall mass transfer coefficient of VC into the water film (K_L) with temperature.

due to the fact that the r_L decreases, while the r_G increases with temperature. The excessively high values of the ratios r_L/r_G, indicate that the liquid phase resistance controls the transfer of VC into water.

4.2. Variation with the liquid-free surface area

(1) The diffusion coefficients of VC into nitrogen are independent of the water-free surface area, as the theory predicts. (2) The partition coefficients of VC between the water at the interface and nitrogen, *K*, are higher when the water-free surface area is smaller, i.e., $(K)_{\alpha_L} < (K)_{\alpha_L'}$. The latter can be explained as follows: as $(K)_{\alpha_L} = (c_{L(int)})_{\alpha_L}/(c_G)_{\alpha_L}$ and $(K)_{\alpha_L'} = (c_{L(int)})_{\alpha_L'}/(c_G)_{\alpha_L'}$, where $c_{L(int)}$ and c_G are the equilibrium concentrations of VC at the water interface and nitrogen, respectively, and $(c_G)_{\alpha_L} =$

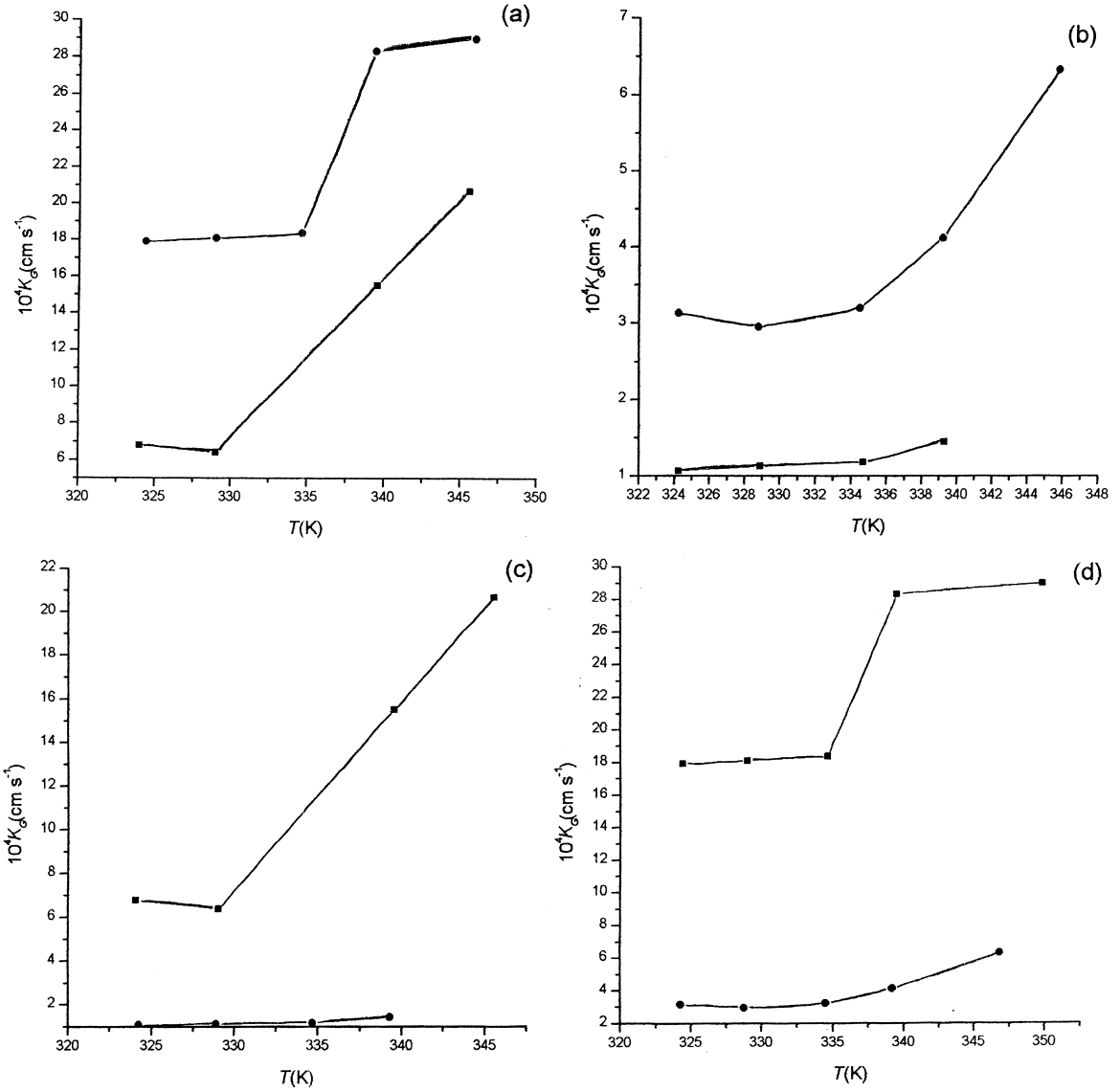

Fig. 8. Variation of overall mass transfer coefficient of VC into the nitrogen film (K_G) with temperature.

$(c_G)_{\alpha_L'}$, as $a_G = a_G'$, it is obvious that $(c_{L(int)})_{\alpha_L'} > (c_{L(int)})_{\alpha_L}$, because the same VC quantity is adsorbed in smaller surface area. (3) The partition coefficients of VC between the water bulk and nitrogen, K', are higher when the water surface area is larger, i.e., $(K')_{\alpha_L} > (K')_{\alpha_L'}$, as $(c_{L(bulk)})_{\alpha_L} > (c_{L(bulk)})_{\alpha_L'}$. (4) The partition coefficients of VC between the water at the interface and the bulk, $K'' = K/K'$, are higher when the water-free surface area is smaller, i.e., $K''_{\alpha_L} < K''_{\alpha_L'}$. This is obvious since $(c_{L(int)})_{\alpha_L'} > (c_{L(int)})_{\alpha_L}$ and $(c_{L(bulk)})_{\alpha_L} > (c_{L(bulk)})_{\alpha_L'}$. (5) Even the diffusion coefficients of VC into water, D_L, should be independent of the water-free surface area, our results indicate a variation of D_L with a_L, as $(D_L)_{\alpha_L} > (D_L)_{\alpha_L'}$. The latter can be attributed to the fact that the found D_L values do not express true but apparent diffusion coefficients, which maybe include partition coefficients and mass transfer coefficients. (6) The

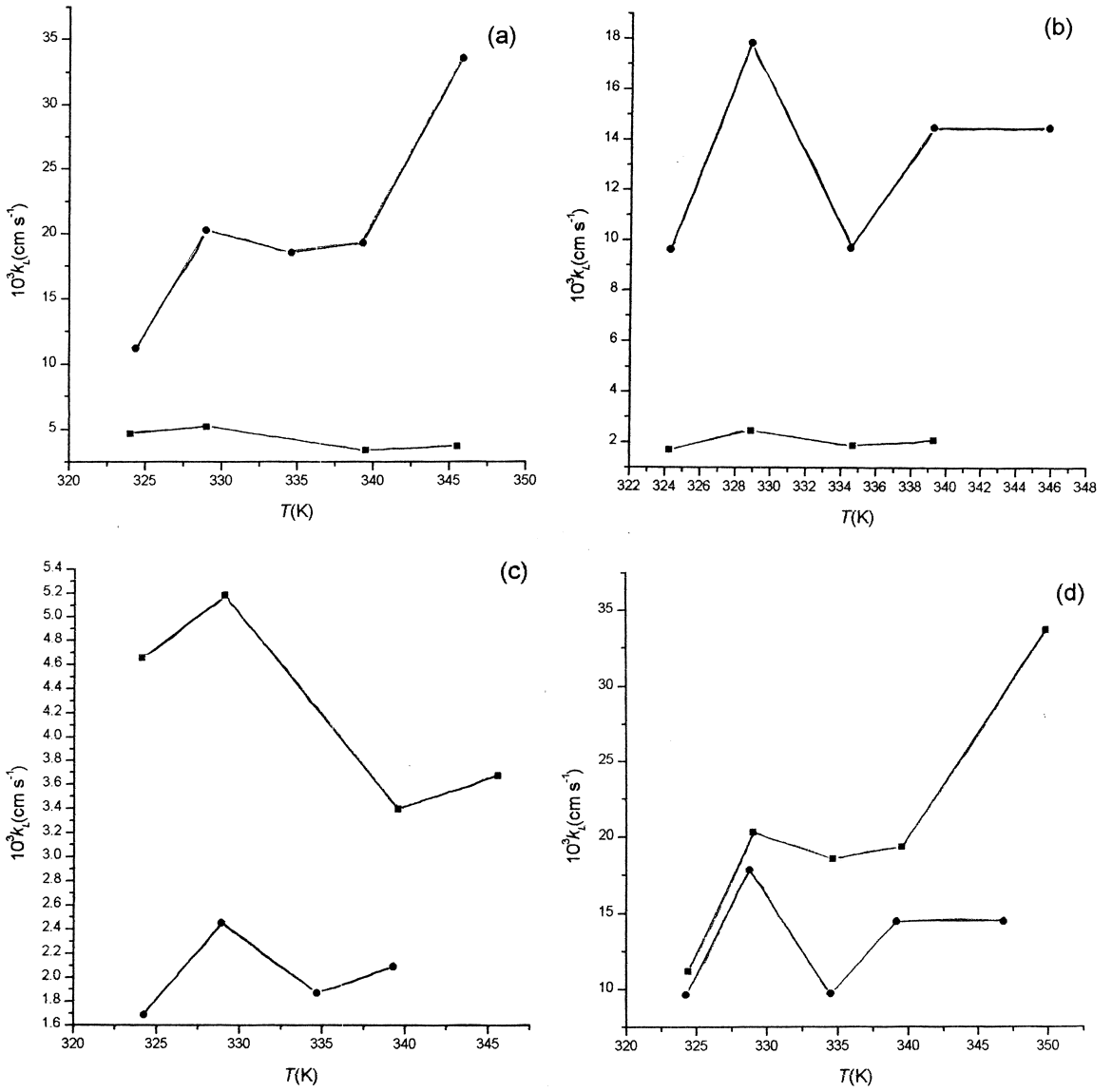

Fig. 9. Temperature dependence of water film transfer coefficient (k_L) for the transfer of VC into water.

overall mass transfer coefficients of VC in the water phase, K_L, are lower when the water-free surface area is larger, i.e., $(K_L)_{\alpha_L} < (K_L)_{\alpha_L'}$, as K_L is inversely proportional to a_L ($K_L = \pi^2 D_L V_L / 4L^2 a_L$). The same holds for the water film transfer coefficients of VC, k_L. (7) The overall mass transfer coefficients of VC in the gas (nitrogen) phase, K_G, decrease with increasing the water-free surface area, i.e., $(K_G)_{\alpha_L} < (K_G)_{\alpha_L'}$, as K_G is inversely proportional to a_L ($K_G = k_G a_G / a_L$). (8) As a consequence of conclusions (6) and (7), the liquid phase resistances, r_L, increase with increasing a_L, as $r_L = 1/k_L$. The same holds for the gas phase resistances, r_G, because $r_G = K'/k_G$ and $(K')_{\alpha_L} > (K')_{\alpha_L'}$. The ratios of the liquid to the gas phase resistances of VC, r_L/r_G, are higher when the water-free surface area is larger. (9) The thick-

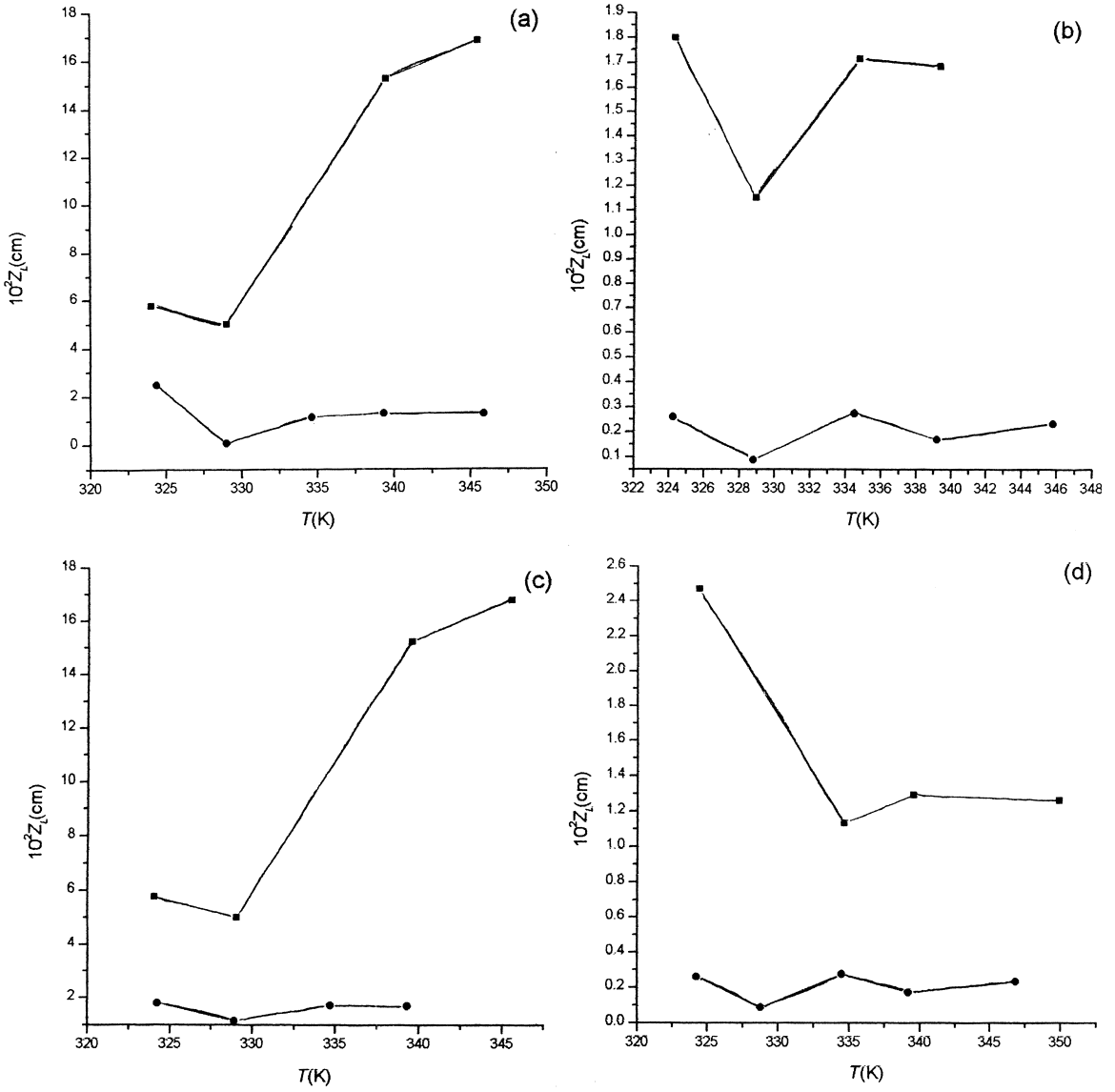

Fig. 10. Temperature dependence of the thickness of the stagnant film in water (z_L) for the transfer of VC into water.

ness of the stagnant film of VC in water, z_L, increases with increasing a_L, i.e., $(z_L)_{\alpha_L} > (z_L)_{\alpha'_L}$, as $z_L = D_L/k_L$ and $(D_L)_{\alpha_L} > (D_L)_{\alpha'_L}$, $(k_L)_{\alpha_L} < (k_L)_{\alpha'_L}$.

4.3. Variation with the liquid volume

(1) The diffusion coefficients of VC into nitrogen, are independent of the water volume, according to the theory. (2) The partition coefficients of VC between the water at the interface and nitrogen, K, are lower when the volume of water is larger, i.e., $(K)_{V_L} < (K)_{V'_L}$, because $(c_{L(int)})_{V_L} < (c_{L(int)})_{V'_L}$. The same unequality holds also for the partition coefficients of VC between the water bulk and nitrogen, i.e., $(K')_{V_L} < (K')_{V'_L}$. Finally, the partition coefficients of VC between the water at the interface and the bulk, K'', increase with the volume of water,

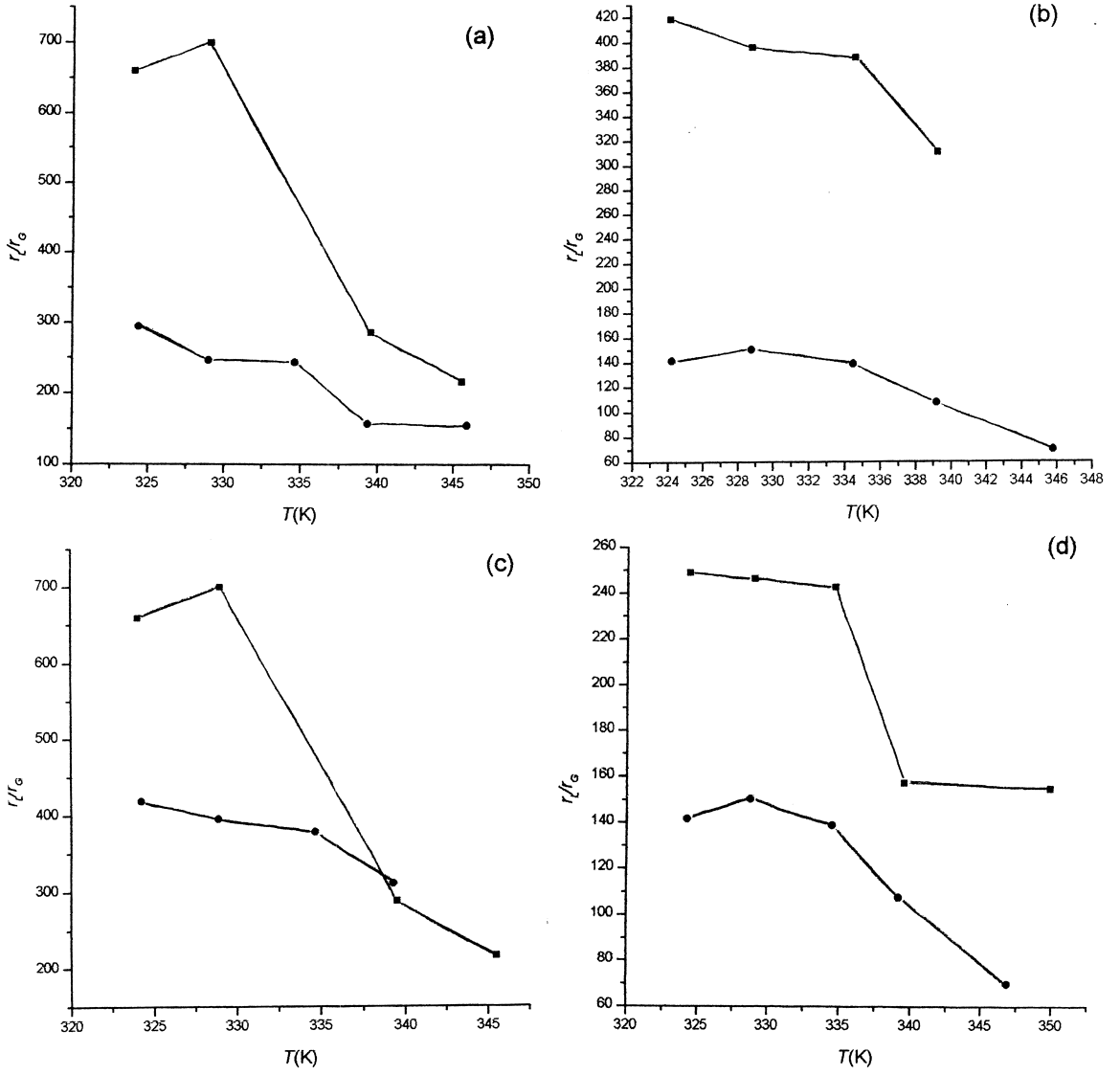

Fig. 11. Temperature dependence of the ratio of the water (r_L) and nitrogen (r_G) resistances (r_L/r_G) for the transfer of VC into water.

due to the reason that the ratio $(K')_{V_L'}/(K')_{V_L}$ is larger than the ratio $(K)_{V_L'}/(K)_{V_L}$. (3) The diffusion coefficients of VC into water, D_L, except from some cases which can be attributed to accidental errors, are independent of the volume of water. (4) The overall mass transfer coefficients of VC in the water phase, K_L, increase with increasing the liquid volume, i.e., $(K_L)_{V_L} > (K_L)_{V_L'}$, as K_L is proportional to V_L, according to the relation: $K_L = \pi^2 D_L V_L / 4L^2 a_L$. The same unequality holds for the parameters k_L, i.e., $(k_L)_{V_L} > (k_L)_{V_L'}$. (5) The overall mass transfer coefficients of VC in the nitrogen phase, K_G, increase with decreasing the water volume, as $(K'_L)_{V_L'}/(K'_L)_{V_L} > (K_L)_{V_L}/(K_L)_{V_L'}$. (6) According to conclusions (4) and (5) mentioned previously, the resistances in the liquid and gas phases for the transfer of VC into water follow the order: $(r_L)_{V_L} < (r_L)_{V_L'}$ and $(r_G)_{V_L} < (r_G)_{V_L'}$. Due to the fact that $(r_G)_{V_L'}/(r_G)_{V_L} > (r_L)_{V_L'}/(r_L)_{V_L}$, the

ratios r_L/r_G follow the order: $(r_L/r_G)_{V_L} > (r_L/r_G)_{V_L'}$. (7) The thickness of the stagnant film of VC in water, z_L decreases with increasing V_L, i.e. $(z_L)_{V_L} < (z_L)_{V_L'}$, as $(k_L)_{V_L}/(k_L)_{V_L'} > (D_L)_{V_L}/(D_L)_{V_L'}$.

4.4. Comparative study

(1) Comparison of the experimental diffusion coefficients of VC into nitrogen with those calculated theoretically by using the Fuller–Schettler–Giddings equation [27] shows a deviation of about 7%. (2) The experimental diffusion coefficients of VC into water are of the same order and in some cases very close to those calculated from the equation of Wilke-Chang [28]. (3) The liquid film transfer coefficients of VC into water, found in the present work, are of the same order and in some cases very close to the value $k_L = 4.66 \cdot 10^{-3}$ cm s^{-1} given in Ref. [1]. The same holds also for the ratios of the two resistances in the liquid and the gas films, r_L/r_G. (4) The values of the thickness of the stagnant film in the liquid phase for the transfer of VC into water, found in the present work, are of the same order and in some cases very close to the corresponding value for the transfer of oxygen into water given in Ref. [1] ($z_{L(O_2)} = 4 \cdot 10^{-3}$ cm).

5. Conclusions

The present work resulted in the following conclusions:

(i) The reversed-flow gas chromatography technique can be used with simplicity and accuracy for the study not only of the distribution of a gas between a gaseous and a liquid phase, but also for the flux of the gas across the gas–liquid interface. Using suitable mathematical analysis, equations were derived by means of which the relevant physicochemical quantities describing the thermodynamics and the kinetics of the above processes were calculated.

(ii) The free surface area and the volume of the liquid (water) influence the mass transfer coefficients of the gases across the air–water interface, indicating that in the design of suitable systems for adsorption of gases by liquids, these parameters play an important role.

(iii) Comparison of the experimental results found in the present work with those calculated theoretically or found in literature, shows, in some cases, very good accuracy of the proposed method.

(iv) In all experiments, the liquid phase resistance controls the transfer of vinyl chloride into water and the rate determining step for the adsorption of VC by quiescent water is the transfer of VC from the water interface to the water bulk.

Acknowledgements

The authors thank Mrs. M. Barkoula for technical assistance. K.R.A. is grateful to the Greek State Scholarships Foundation for the scholarship.

References

[1] P.S. Lis, P.G. Slater, Nature 247 (1974) 181.
[2] D. Mackay, in: W.B. Neely, U.E. Blau (Eds.), Environmental Exposure from Chemicals, Vol. 1, CRC Press, Boca Raton, FL, 1985, Chapter 5.
[3] D. Mackay, J. Great Lakes Res. 8 (1982) 299.
[4] D.A. Blackadder, R.M. Nedderman, in: Handbook of Unit Operations, Academic Press, New York, 1971.
[5] N.A. Katsanos, G. Karaiskakis, Adv. Chromatogr. 24 (1984) 125.
[6] D. Gavril, G. Karaiskakis, Instrum. Sci. Technol. 25 (1997) 217.
[7] D. Gavril, G. Karaiskakis, Chromatographia 47 (1998) 63.
[8] N.A. Katsanos, E. Dalas, J. Phys. Chem. 91 (1987) 3103.
[9] N.A. Katsanos, J. Kapolos, Anal. Chem. 61 (1989) 2231.
[10] N.A. Katsanos, G. Karaiskakis, J. Chromatogr. 237 (1982) 1.
[11] N.A. Katsanos, G. Karaiskakis, J. Chromatogr. 254 (1983) 15.
[12] G. Karaiskakis, N.A. Katsanos, A. Niotis, J. Chromatogr. 235 (1982) 21.
[13] G. Karaiskakis, N. Niotis, N.A. Katsanos, J. Chromatogr. Sci. 22 (1984) 554.
[14] G. Karaiskakis, J. Chromatogr. Sci. 23 (1985) 360.
[15] N.A. Katsanos, G. Karaiskakis, P. Agathonos, J. Chromatogr. 349 (1986) 369.
[16] P. Agathonos, G. Karaiskakis, J. Appl. Polym. Sci. 37 (1989) 2237.
[17] N.A. Katsanos, G. Karaiskakis, J. Catal. 94 (1985) 376.
[18] D. Gavril, A. Koliadima, G. Karaiskakis, Chromatographia 49 (1999) 285.
[19] D. Gavril, N.A. Katsanos, G. Karaiskakis, J. Chromatogr. A 852 (1999) 507.

[20] D. Gavril, A. Koliadima, G. Karaiskakis, Langmuir 15 (1999) 3798.
[21] D. Gavril, G. Karaiskakis, J. Chromatogr. A 845 (1999) 67.
[22] N.A. Katsanos, R. Thede, F. Roubani-Kalantzopoulou, J. Chromatogr. A 795 (1998) 133.
[23] N.A. Katsanos, F. Roubani-Kalantzopoulou, Adv. Chromatogr. 40 (2000) 231.
[24] S.G. Gilbert, J. Food Sci. 41 (1976) 955.
[25] J.R. Marono, J.R. Giacin, S.G. Gilbert, J. Food Sci. 42 (1977) 230.
[26] N.A. Katsanos, F. Roubani-Kalantzopoulou, J. Chromatogr. A 710 (1995) 191.
[27] E.N. Fuller, P.D. Schettler, J.C. Giddings, Ind. Eng. Chem. 58 (1966) 19.
[28] J.C. Giddings, in: Dynamics of Chromatography, Marcel Dekker, New York, 1965.